Journal of Biomedical Materials Research Part A

WILEY

Society For Biomaterials

RESEARCH ARTICLE OPEN ACCESS

Biofabrication and Characterization of Vascularizing PEG-Norbornene Microgels

Nicole E. Friend[1] | Irene W. Zhang[1] | Michael M. Hu[1] | Atticus J. McCoy[1] | Robert N. Kent III[1] | Samuel J. DePalma[1] | Brendon M. Baker[1,2] | Sasha Cai Lesher-Pérez[1,2] | Jan P. Stegemann[1] | Andrew J. Putnam[1]

[1]Department of Biomedical Engineering, University of Michigan, Ann Arbor, Michigan, USA | [2]Department of Chemical Engineering, University of Michigan, Ann Arbor, Michigan, USA

Correspondence: Jan P. Stegemann (jpsteg@umich.edu) | Andrew J. Putnam (putnam@umich.edu)

Received: 17 December 2024 | **Revised:** 4 March 2025 | **Accepted:** 8 March 2025

Funding: Research reported in this publication was supported by the National Heart, Lung, and Blood Institute of the National Institutes of Health under Award Numbers R01-HL085339 (A.J.P.) and R01-HL118259 (J.P.S. and A.J.P.). N.E.F. was partially supported by the Tissue Engineering and Regeneration Training Program at the University of Michigan (T32-DE007057) and the Rackham Merit Fellowship. I.W.Z. was partially supported by the Cellular Biotechnology Training Program at the University of Michigan (T32-GM145304). A.J.M. was partially supported by the Training Program in Translational Cardiovascular Research and Entrepreneurship at the University of Michigan (T32-HL125242). The content is solely the responsibility of the authors and does not necessarily represent the official views of the National Institutes of Health.

Keywords: microfluidics | microgels | poly(ethylene glycol) | prevascularization

ABSTRACT

Establishing a robust, functional microvascular network remains a critical challenge for both the revascularization of damaged or diseased tissues and the development of engineered biological materials. Vascularizing microgels may aid in efforts to develop complex, multiphasic tissues by providing discrete, vascularized tissue modules that can be distributed throughout engineered constructs to vascularize large volumes. Here, we fabricated poly(ethylene glycol)-norbornene (PEGNB) microgels containing endothelial and stromal cells via flow-focusing microfluidic droplet generation. When embedded in bulk fibrin hydrogels, these cell-laden microgels initiated the formation and development of robust microvascular networks. Furthermore, extended preculture of cell-laden PEGNB microgels enabled the formation of vessel-like structures supported by basement membrane within the matrix without aggregation. Our findings highlight the suitability of PEG-based matrices for the development of vascularizing microgels capable of forming well-distributed, robust microvascular networks.

1 | Introduction

Traditional tissue engineering strategies typically involve seeding cells within scaffolds or encapsulating them within hydrogels [1]. However, engineering large, functional tissue replacements to overcome the persistent problem of organ shortages has proven difficult for more than 25 years, primarily due to the inability to provide adequate vascularization throughout constructs manufactured via these traditional approaches [2, 3]. Similarly, creating functional microvasculature throughout large volumes to restore perfusion to ischemic tissues remains an ongoing challenge.

Strategies based on the assembly of small modular tissues (i.e., microgels, microspheres, microparticles, microbeads, etc.) have emerged as a promising approach to building larger tissues. For example, granular hydrogels, including microporous annealed particle (MAP) scaffolds, are comprised of crosslinked micron-sized microgels with an interconnected pore structure formed by the void spaces between microgels [4]. These granular materials

are inherently modular, as they can be composed of diverse, heterogeneous populations of microgels [5]. Though typically composed of acellular microgel building blocks, the individual modules are small enough (100–300 μm) to enable encapsulated cells to survive and function based on oxygen and nutrient diffusion alone. Discrete cell-laden modules comprising unique microenvironments can be fabricated, cultured in tissue-specific media, and then delivered in a minimally invasive fashion as functional tissue units or combined to engineer complex, multiphasic tissue structures [5, 6]. Cell-laden microgels have also been developed as extrudable inks for bioprinting [7–9] and as components of supportive baths for extrusion printing [10–12].

Vascularizing microgels are of particular interest as they could be incorporated into either granular and/or 3D bioprinted scaffolds to increase the functionality and complexity of multiphasic engineered tissues and to potentially nucleate the formation of more extensive vasculature. Previous studies have developed microgels that support the in vitro culture [13–16] and in vivo delivery of endothelial cells [17–21]; however, only a small number of these studies focused on vascularization within these microgels [20, 22–26], all of which utilize (modified) natural matrices. Previous work from our groups developed cellularized fibrin-based microgels that support prevascularization in vitro and the formation of functional microvascular networks in vivo after implantation in subcutaneous [26] and hindlimb ischemia [25] models. While these studies demonstrated a promising modular approach to vascularizing ischemic tissues, the animal origins of many natural materials and their batch-to-batch variability may be barriers to translation. Furthermore, fibrin microgels were prone to aggregation when cultured in suspension for extended periods of time in order to achieve prevascularization [15, 25, 26]. This resulted in heterogeneous populations of microgels with diameters greater than 400 μm (larger than the estimated diffusion limitation in many tissues [27]) which could limit nutrient diffusion, hinder their injectability or printability, and reduce the overall distribution of the microvasculature throughout tissue constructs.

Poly(ethylene glycol) (PEG) has been widely explored as a promising material for tissue engineering applications due to its ability to be modified with specific end groups to confer desired biological functionalities, affording relatively easy customization of hydrogel properties [28]. PEG-based hydrogels have a demonstrated ability to support microvascular networks in vitro [29–32] and in vivo [33]. Acellular PEG microgels have also been established for biomolecule delivery [34–36] and as building blocks for larger hydrogel scaffolds formed either via jamming [37] or secondary crosslinking to create MAP hydrogels [4]. Previous literature has demonstrated the encapsulation of endothelial cells within PEG-based microgels, focusing mainly on cell viability [16, 38] and subsequent injection in vivo [18, 19]. However, the prevascularization of synthetic microgels through a period of in vitro preculture prior to delivery, which may aid in the rapid development of mature, functional microvasculature, has not been investigated. To address this gap, in this study, we first fabricated cell-adhesive, degradable PEG-norbornene (PEGNB) microgels containing endothelial and stromal cells. We then evaluated their ability to support vessel morphogenesis within individual microgels, reduce microgel aggregation, and nucleate the formation of robust, well-distributed microvascular networks.

2 | Materials and Methods

2.1 | Cell Culture

Human umbilical vein endothelial cells (HUVECs) were isolated from umbilical cords from the University of Michigan Mott Children's Hospital as previously described [39]. Umbilical cords were obtained by a process considered exempt by the University of Michigan's Institutional Review Board (notice of determination dated August 21, 2014) because the tissue is normally discarded, and no identifying information is provided to the researchers who receive the cords. HUVEC were cultured in fully supplemented EGM2 (Lonza Inc., Walkersville, MD). HUVEC were used from passages 4 to 7. Normal human lung fibroblasts (NHLFs; Lonza) were cultured in Dulbecco's modified Eagle's medium (DMEM; Gibco, Waltham, MA) supplemented with 10% fetal bovine serum (FBS; Gibco). NHLF were used from passages 10 to 15. All cells were cultured at 37°C and 5% CO_2 with media replacement every 2 days.

2.2 | Microfluidic Droplet Generation of PEGNB Microgels

PEGNB microgels were formed via thiol–ene photopolymerization. PEGNB (4-arm, 20 kDa; Creative PEGWorks, Durham, NC) and lithium phenyl-2,4,6-trimethylbenzoylphosphinate (LAP; Sigma-Aldrich, St. Louis, MO) were purchased from commercial sources that provide the percent substitution of norbornene by NMR and purity by HPLC, respectively. The thiol-containing adhesive peptide Ac-CGRGDS-NH2 (RGD; AAPPTEC, Louisville, KY) and dithiol-containing matrix metalloproteinase- (MMP-) sensitive crosslinking peptide Ac-GCRDVPMS↓MRGGDRCG-NH2 (VPMS, cleavage site indicated by ↓; AAPPTEC), which contain an N-terminal acetylation and a C-terminal amidation, were dissolved in 25 mM acetic acid, filtered through 0.22 μm filters (Sigma-Aldrich), lyophilized for 48 h, and stored in a desiccator at −20°C. The thiol content (purity) of each batch of peptide aliquots was determined using Ellman's reagent (Thermo Fisher, Waltham, MA). PEGNB and LAP were suspended in serum-free EGM2 (SF-EGM2) and sterile filtered through 0.22 μm filters to create fresh stocks at desired concentrations for each experiment. Sterile peptides were resuspended in SF-EGM2 to reach desired concentrations.

A flow-focusing microfluidic device was used to encapsulate cells in PEGNB microgels. The discontinuous phase consisted of 20×10^6 total cells/mL in a 1:1 HUVEC:NHLF ratio suspended in a precursor solution comprised of 3 wt% PEGNB (w/v), 0.1 wt% LAP (w/v), 0.1% Pluronic F-68 (v/v; Gibco), 1 mM RGD, 2.25 mM VPMS (90% crosslinked, 0.9 thiols per norbornene after accounting for RGD concentration), and SF-EGM2. Monoculture microgels contained 20×10^6 total cells/mL of each individual cell type. The continuous phase consisted of sterile filtered 0.5% FluoroSurfactant (008-FluoroSurfactant; RAN Biotechnologies, Beverly, MA) in NOVEC-7500 (Best Technology Inc., Minneapolis, MN). Microgel precursor solutions and fluorinated oil were loaded into glass syringes (Hamilton Company, Reno, NV) and injected into the microfluidic device via syringe pumps at constant flow rates of 15 and 30 μL/min, respectively. The syringe containing the cellular

precursor solution was placed vertically and contained a small magnetic stir bar (6 mm × 3 mm; Big Science Inc., Huntersville, NC), which was continuously stirred using an adjacent stir plate to prevent cell settling throughout droplet generation. Microgels were collected in a single well of a standard 24-well plate and polymerized with a 6-W LED 365 nm Gooseneck Illuminator (AmScope, Feasterville, PA) placed 1.5 in. above the microgels and set to max intensity for 90 s, corresponding to approximately 50 mW/cm^2 as measured by a radiometer.

Microgels were collected from the oil via sequential on-strainer rinses. First, microgels were rinsed three times with DMEM containing 10% FBS and 1% Pluronic F-68 on a 40 μm cell strainer (Fisher). Then, microgels were rinsed three times with DMEM containing 10% FBS on the strainer. Microgels were transferred to a vented 50 mL conical tube with a filter cap (CELLTREAT Scientific Products, Shirley, MA) containing 20 mL of warm EGM2. Microgel suspensions were cultured under static conditions for up to 7 days. The medium was changed the day after, then every other day. During medium changes, the spent medium was aspirated from above the settled microgel pellet, and then the microgels were disturbed and redistributed upon the addition of new medium.

2.3 | Mechanical Characterization of Bulk PEGNB Hydrogels

Hydrogel shear storage moduli (G′) were measured on Day 1 (after overnight swelling) for bulk hydrogels of the same formulation (chemical composition and cell density) as microgels. Hydrogels were centered between the Peltier plate and an 8-mm measurement head of an AR-G2 rheometer (TA Instruments, New Castle, DE). The Peltier plate and measurement head were covered with P800 sandpaper to reduce slippage. Shear storage modulus was averaged over a 1-min time sweep measured at 37°C, 5% strain amplitude, 1 rad/s frequency, and either 0.05 N normal force or a minimum gap height of 1000 μm, if hydrogels were too soft to reach the target normal force. In situ rheology to measure gelation kinetics of 300 μL bulk hydrogels upon UV exposure was performed using a 5-min time sweep at 5% strain amplitude and 1000 μm gap height in which the UV light (50 mW/cm^2) was turned on at 30 s.

2.4 | Angiogenesis Assay

Microgels cultured for 1 day (D1 PC) were embedded in bulk fibrin hydrogels to evaluate angiogenic sprouting, similar to models previously described [40, 41]. Culture media above the settled microgels were aspirated, leaving only microgels in a small volume of media. Precursor solutions were made by mixing varying volumes of microgels with SF-EGM2, FBS (10% final), thrombin (1 U/mL final), and fibrinogen stock solution (2.5–10.0 mg/mL final clottable protein). For HUVEC monoculture microgels embedded with stromal cells in the surrounding fibrin, 250 K/mL NHLF were also included in the precursor solution. Then, 500 or 250 μL of the microgel-protein mixture was added per well of a standard 24- or 48-well culture plate, respectively, and incubated at room temperature for 5 min before being placed in the incubator for 25 min at 37°C to complete the gelation process. EGM2 (0.5–1 mL/well) was added to each hydrogel after gelation. Media were changed the day after, then every other day for 7 days.

2.5 | Imaging and Quantification

After overnight swelling, quantification of microgel diameter and cell density was performed on 4X brightfield images using Fiji. Cell densities per microgel are reported based on the fractional area occupied by cell bodies in individual microgel images and binned into four categories representing > 50% (high), 25%–50% (medium), < 25% (low), or none (empty) of the microgel occupied by cells. Polydispersity index (PDI) was calculated as PDI = (standard deviation/mean)^2. Viability of cells encapsulated in the microgels was assessed using a Live/Dead Cell Imaging Kit (Fisher: Invitrogen). On Days 1, 3, 5, or 7, microgels in suspension and fibrin hydrogels were fixed with zinc formalin (Z-fix; Anatech, Battle Creek, MI) for 10 min, then washed three times with 1X Tris-buffered saline (TBS) for 5 min. Hydrogels were stained overnight with rhodamine-conjugated lectin from *Ulex europaeus* agglutinin I (UEA, 1:200; Vector Laboratories, Newark, CA), 4′,6-diamidino-2-phenylindole (DAPI, 1 μg/mL; Thermo Fisher), and AlexaFluor 488 phalloidin (1:200; Thermo Fisher) which label endothelial cells, cell nuclei, and F-actin, respectively. Samples were rinsed overnight with TBS prior to imaging. For immunofluorescent staining of basement membrane proteins, samples were permeabilized with 0.5% (v/v) Triton X-100 (Thermo Fisher) in TBS for 1 h, rinsed four times for 5 min with 0.1% (v/v) Tween-20 (Thermo Fisher) in TBS (TBS-T), and blocked overnight at 4°C in antibody diluting (AbDil) solution consisting of 2% (w/v) bovine serum albumin (BSA; Sigma-Aldrich) in TBS-T. Gels were incubated with primary antibodies for collagen IV (1:500, mouse IgG1; Thermo Fisher) or laminin beta-1 (1:500, rabbit IgG; Thermo Fisher) diluted in AbDil solution overnight at 4°C. Gels were washed three times for 5 min and rinsed overnight at 4°C with TBS-T. Gels were stained with appropriate secondary antibodies, AlexaFluor 488 goat anti-mouse (1:200, IgGH+L; Thermo Fisher) or AlexaFluor 488 goat anti-rabbit (1:200, IgGH+L; Thermo Fisher), diluted in TBS-T and UEA and DAPI, as described above, overnight at 4°C. Gels were rinsed overnight at 4°C with TBS-T prior to imaging. Confocal z-stacks (4X, 10X, 20X, 40X) and scan slides (4X) were acquired using an Olympus IX81 microscope equipped with a disk-scanning unit (DSU; Olympus America, Center Valley, PA) and Metamorph Premier software (Molecular Devices, Sunnyvale, CA). Z-series stacks were collapsed into maximum intensity projections using Fiji. Quantification of preformed microvascular structures within precultured microgels was performed on 150 μm stacks (25 μm/slice, 7 slices/stack) imaged at 4X magnification. Total vessel length (the cumulative sum of vessel-like segments, in mm) in 4X scan slides was quantified using the angiogenesis tube formation module in Metamorph.

2.6 | Statistics

Statistical analysis was performed using Prism (GraphPad, La Jolla, CA). Data are represented as mean ± standard deviation of at least three independent experimental replicates. Data were checked for normality using a Shapiro–Wilk test

($p > 0.05$) before statistical analyses. Data were analyzed using one-way ANOVA with Tukey post hoc testing with prespecified comparisons between conditions. A value of $p \leq 0.05$ was considered significant.

3 | Results and Discussion

3.1 | Microfabrication of Cell-Adhesive, Degradable PEGNB Microgels Containing Endothelial and Stromal Cells

A flow-focusing microfluidic device was used to produce cell-laden PEGNB microgels (Figure 1). While there is an established body of literature surrounding PEG-based microgels, comparatively fewer studies encapsulate cells within the microgel matrix, and even fewer do so via microfluidic droplet generation (compared to electrosprayed or batch emulsification methods) [16, 18, 42]. Microgel composition was selected based upon our prior work vascularizing bulk PEGNB hydrogels [43]. In fully synthetic PEG hydrogels, RGD (CGRGDS), a fibronectin mimetic adhesive ligand, allows cells to interact with the surrounding matrix, and VPMS (GCRDVPMS↓MRGGDRCG), an MMP-susceptible crosslinker, permits degradation of the matrix via cell-secreted proteases. We have previously shown that the formulation of hydrogel used here (3 wt% PEGNB, 1 mM RGD, 0.9 thiols/norbornene) supports vascularization of bulk gels [43]. The oil phase, flow rates, initial cell concentration, buffers, microgel polymerization, and isolation protocol were varied to improve cell encapsulation efficiency and post-encapsulation viability. Mineral oil with Span-80 (2%–5%) was ineffective in preventing coalescence of low (< 5%) wt% PEGNB microgels during fabrication; therefore, fluorinated oil with a PTFE-based surfactant was used due to its ability to effectively stabilize emulsions [44] as well as its biocompatibility [45]. To improve the cell distribution in the microgels, a small stir bar was added to the glass syringe containing the precursor solution before it was loaded on a vertically oriented syringe pump adjacent to a small stir plate. The solution was continuously stirred throughout droplet production to prevent cell settling in the syringe. Microgels were crosslinked off the microfluidic device via bulk exposure to UV for complete polymerization. Initial attempts to photopolymerize low wt% PEGNB microgels in an adjacent PDMS-glass serpentine channel exposed to UV prior to collection were unsuccessful. Though 10 and 5 wt% PEGNB microgels could be crosslinked in 30 and 60 s, respectively, within the serpentine channel, 3 wt% microgels did not polymerize even after extended UV exposure (tested up to 8.5 min). Further, reducing flow rates to increase residence time of UV exposure increased the potential for droplet coalescence. Acellular bulk hydrogels of the same formulation rapidly crosslinked in response to UV exposure, as demonstrated by in situ rheology (Figure 2A).

Cell densities ranging from 4 to 30 million total cells/mL and flow rates ranging from 5:10 to 70:210 μL/min (PEG:oil) were explored to balance increasing the overall number of cell-laden droplets, reducing the time before the precursor solution reached the microfluidic device to prevent cell aggregation, and maintaining continuous, stable droplet production (Figure S1). Higher cell concentrations resulted in a greater number of cell-laden droplets; however, at lower flow rates, greater cell concentration elicited cell aggregation, junction clogging, and unstable droplet production. Higher flow rates allowed for faster droplet production, reducing overall cell aggregation, but also resulted in unstable droplet production and increased droplet polydispersity. Ultimately, utilizing "intermediate" flow rates of 15:30 μL/min (precursor:oil) and a cell concentration of 20 million total cells/mL produced the greatest incidence of cell-laden microgels while maintaining stable droplet production. Finally, the protocol for isolating the microgels from the perfluorinated oil was optimized to (1) preserve microgel structure by using on-strainer rinses instead of high-speed centrifugation and (2) improve cell viability by using serum-containing media for the rinses as opposed to PBS. Resuspending all microgel precursor components (i.e., PEGNB, LAP, RGD, VPMS, and the cells) in serum-free media also greatly improved post-encapsulation cell viability compared to PBS.

After overnight swelling, referred to as day 1 precultured (D1 PC), microgels had an average diameter of 234.6 ± 37.8 μm (Figure 2B). Cell-laden bulk hydrogels of the same formulation and cell density (20 M/mL) had an average swollen shear storage modulus (G′) of 107.6 ± 14.0 Pa, which falls within the range of stiffnesses previously identified to support vascularization in bulk PEGNB hydrogels [43]. Cell density per microgel was quantified as high, medium, low, or empty if greater than 50%, between 25% and 50%, less than 25%, or none of the microgel was occupied by cell bodies on phase images, respectively (Figure 2C). Roughly half of all microgels had medium (20% ± 2%) or high (31% ± 5%) cell density, with the greatest percentage of microgels (41% ± 2%) having low cell density and a small portion of microgels being empty (9% ± 4%). Microgels contained both fibroblasts and UEA-positive endothelial cells distributed throughout the interior of the microgels (Figure 2D) that displayed high viability 24 h post-encapsulation (Figure 2E). Our group as well as others have demonstrated the ability of NHLF to take on a pericyte-like phenotype and support vessel morphogenesis in vitro and in vivo [26, 41, 43, 46, 47].

Despite variability in cell density as a result of cell aggregation during droplet production, microgels displayed consistent diameters between batches (PDI = 0.03) (Figure 2B). PDI values of 0.1 or less are considered highly monodisperse [48]. Although microfluidic droplet generation enables the production of more monodisperse droplets compared to other methods (e.g., electrospraying, batch emulsification), cell settling and aggregation in the precursor solution at high cell densities often lead to a more variable cell distribution within droplets [49–51]. Therefore, we optimized flow rates and cell concentration in the precursor solution to increase the occurrence of higher cell density microgels without disturbing droplet production (Figure S1), as large cell aggregates can result in flow fluctuations that affect the monodispersity of the droplets [51]. Future iterations of microgels could be produced using other microfluidic geometries that yield larger volumes of microgels in shorter periods of time [52, 53], which may reduce cell aggregation and improve cell distribution across microgels. Nevertheless, ~50% of all microgels contained either a medium or high cell density, which likely possess the threshold density of cells required for vasculogenic

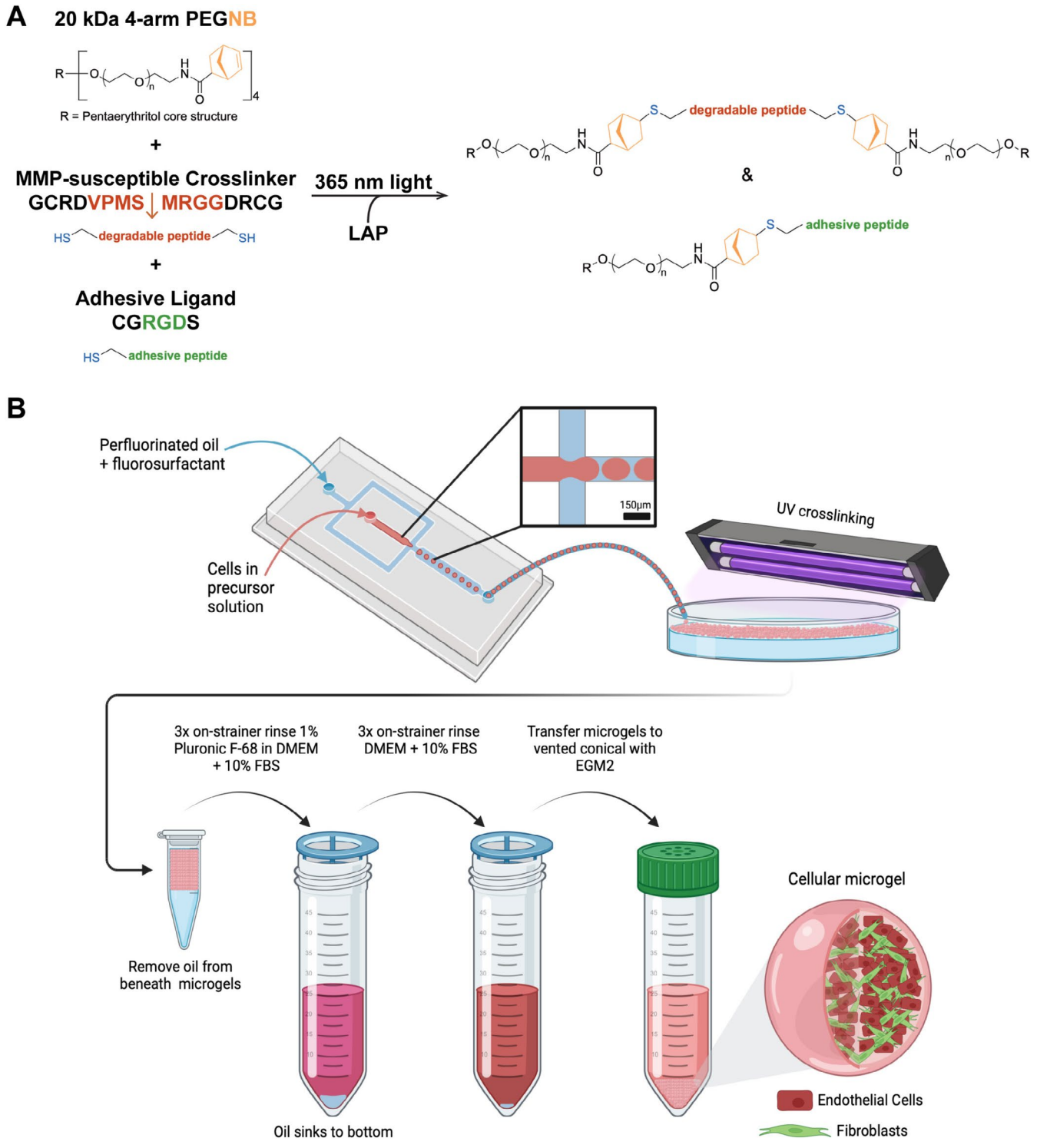

FIGURE 1 | Chemical structures and schematic of microgel fabrication. (A) The microgel precursor solution contained PEGNB and thiol-containing peptides which, in the presence of the photoinitiator LAP, react upon exposure to UV light to form a crosslinked network. (B) Cell-encapsulating microgels were fabricated via flow-focusing microfluidic droplet generation (junction channel width = 150 μm). After off-chip UV crosslinking, microgels were isolated from the oil using repeated on-strainer rinses before being cultured in EGM2 in a vented conical tube. Created with Biorender.com.

assembly. While the other ~50% of the microgels contained only a few or no cells, it is feasible that these low cell density or empty microgels could be beneficial in generating vascularized MAP-like hydrogels [4, 54–56], in which the empty microgels could be utilized for secondary crosslinking if enough free, available norbornene groups remain after microgel polymerization. We recently demonstrated a similar approach in which HUVEC and NHLF co-encapsulated within the void space of PEGNB-based granular hydrogels formed robust microvascular networks throughout the pores of the scaffold in vitro [57].

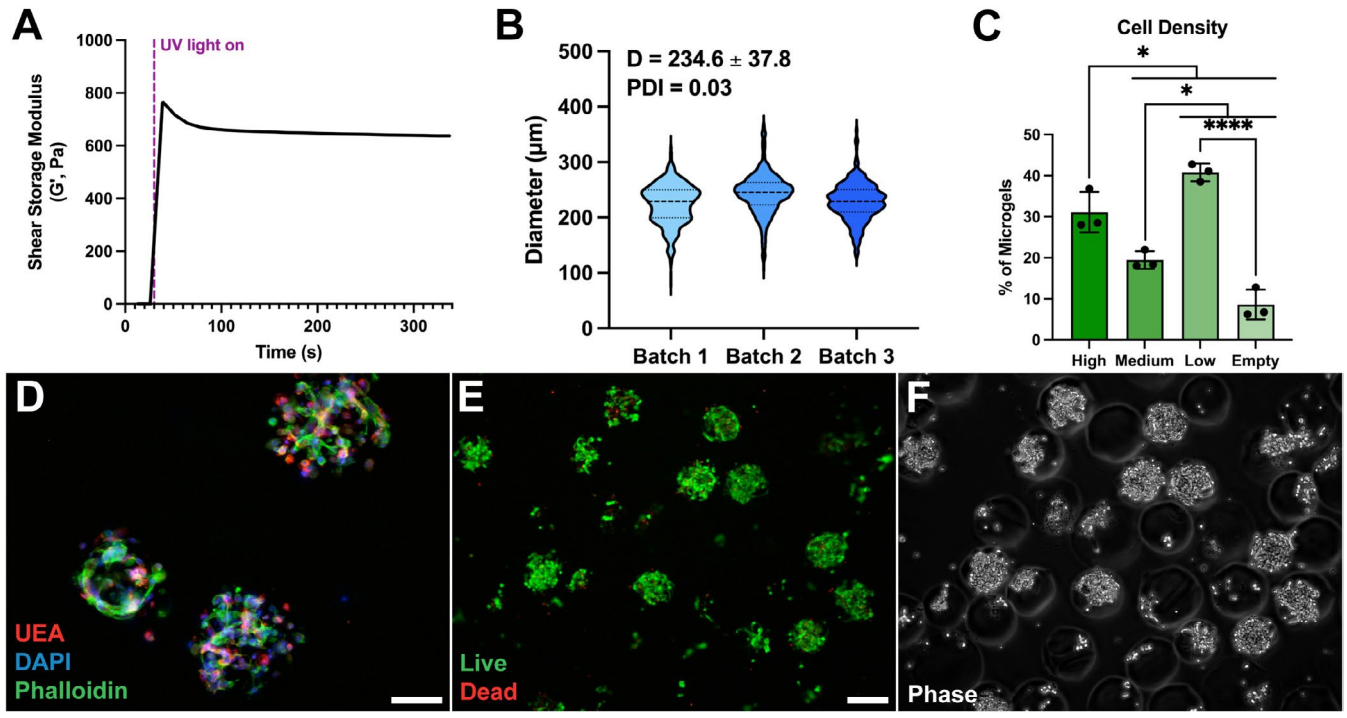

FIGURE 2 | Microgels contained viable endothelial and stromal cells distributed throughout the hydrogel matrix. (A) In situ rheology of acellular bulk hydrogel dynamic crosslinking (UV exposure at 30 s; purple dashed line). (B) Size distribution of cellular microgels. (C) Cell density distribution throughout microgels. (D) Representative max intensity projection ($Z = 150\,\mu m$) of HUVEC and NHLF distributed throughout D1 preculture (PC) microgels (red—UEA, green—phalloidin, blue—DAPI; scale bar = 100 μm). (E) Live/dead staining and (F) phase images of D1 PC microgels (green—live, red—dead; scale bar = 200 μm); *$p < 0.05$, ****$p < 0.0001$, $N = 3$ batches.

3.2 | Microgels Catalyze the Formation of Microvascular Networks in Bulk Fibrin Hydrogels In Vitro

Cellular D1 PC microgels nucleated the formation of microvascular networks when embedded in acellular bulk fibrin hydrogels and cultured for up to 7 days in vitro. After 3 days, 65% ± 8% of cell-laden microgels were surrounded by angiogenic sprouts invading the fibrin matrix, which increased to 82% ± 1% after 7 days. Both vessel structures and stromal cells were present in the surrounding matrix (Figure 3A). The basement membrane component collagen IV (COL IV) was present and localized to UEA-positive vessel structures, indicative of a mature vessel phenotype (Figure 3B). Higher magnification images revealed close perivascular localization of stromal cells, as evident by UEA-negative DAPI and phalloidin staining along the abluminal surfaces of vessel structures (Figure 3C,D). Vessel structures also contained hollow lumens between UEA-positive vessel walls (Figure 3E, arrow).

A robust, interconnected microvascular network will be required to vascularize large tissue volumes. Bulk fibrin hydrogels were loaded with different D1 PC microgel volume fractions to evaluate the required microgel density for well-distributed microvascular networks. All four of the microgel volume fractions evaluated (5%, 10%, 15%, and 20% of the total bulk gel volume) resulted in microvascular networks that were well-distributed throughout the entirety of the hydrogel (diameter = 13 mm). By increasing the volume fraction of microgels encapsulated in bulk fibrin hydrogels, vessel density was increased within the constructs (Figure 4). Including greater than 5% volume fraction of microgels promoted increased vascularization of the surrounding hydrogel (Figure 4E). Modulating vessel density by changing the volume fraction of vascularizing microgels within a construct potentially enables the fabrication of vascular beds that meet the metabolic demands of a variety of tissues [58].

Various biological tissues have differing physical and chemical properties (e.g., stiffness and composition) that control cell behavior and reflect tissue function [59, 60]. D1 PC microgels were embedded in 2.5, 5.0, 7.5, and 10.0 mg/mL fibrin hydrogels to assess how the surrounding matrix density influenced vessel sprouting (Figure 5). Increased fibrin density attenuated overall sprouting, resulting in a 26%, 38%, and 60% reduction in total vessel length in 5.0, 7.5, and 10.0 mg/mL hydrogels, respectively, compared to 2.5 mg/mL fibrin. This is consistent with our previous work showing attenuation of vascular morphogenesis by increasing fibrin density [40]; however, sprouting still occurred in even the highest density fibrin (Figure 5D), which may be important when developing tissues of heterogeneous matrix composition. As fibrin density was increased, vessel structures remained more closely localized to the surface of microgels despite the fibroblasts having invaded into the surrounding matrix.

3.3 | Extended Preculture of Microgels Permits the Formation of Primitive Microvascular Networks Within Individual Microgels

Previous studies have demonstrated varying degrees of prevascularization of discrete microgels ranging from approximately 350–900 μm in diameter using modified natural matrices,

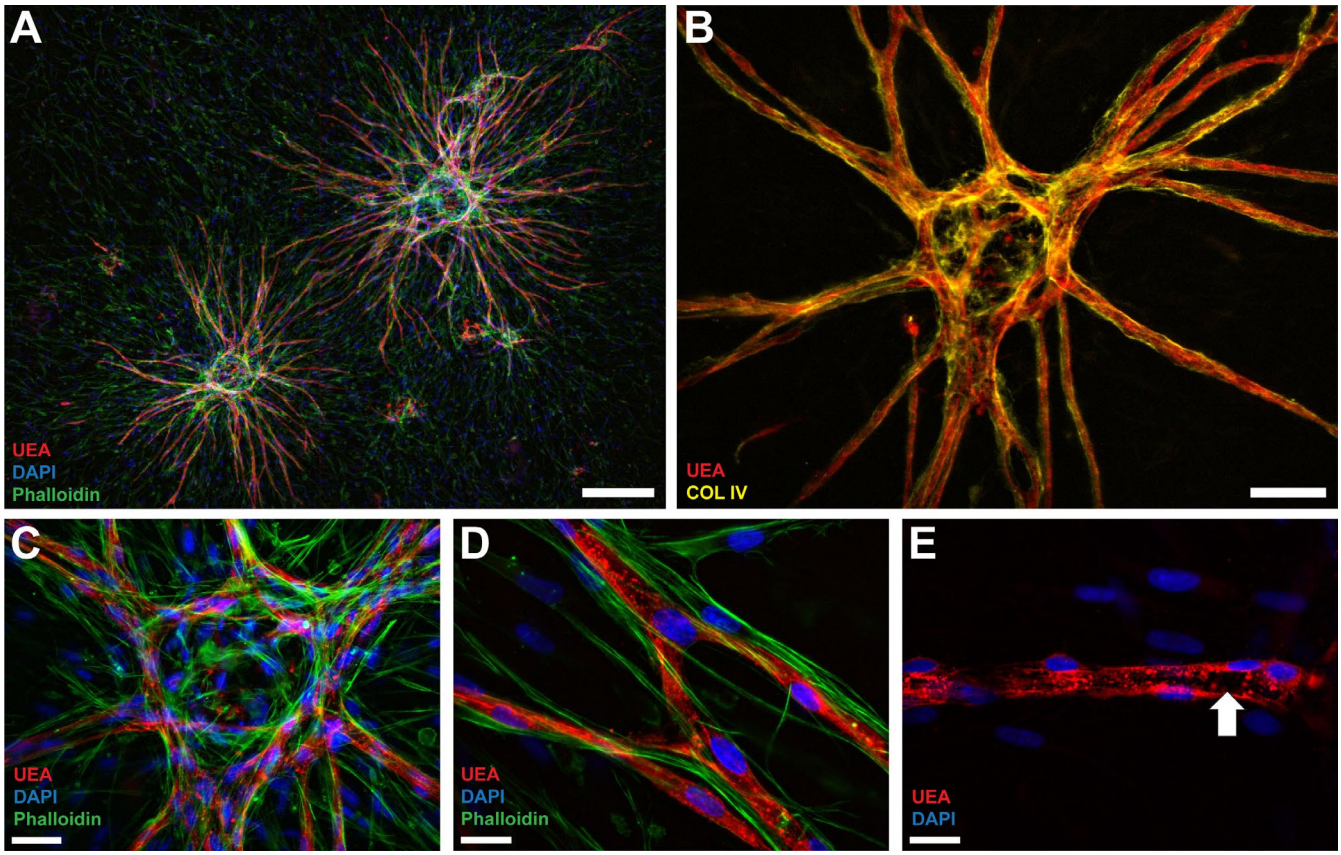

FIGURE 3 | D1 PC microgels vascularize tissue mimics in vitro. (A) Vessel structures and stromal cells sprout from PEGNB microgels after 7 days of culture (scale bar = 500 μm). (B) Basement membrane, COL IV, deposition was localized to vessel structures (scale bar = 100 μm). NHLF were closely associated with vessel structures present (C) near microgels (scale bar = 50 μm) and (D) along vessel sprouts (scale bar = 25 μm). (E) Hollow lumen (arrow) formation was demonstrated through laser confocal microscopy at the middle slice of vessel structures (scale bar = 25 μm) (red—UEA, green—phalloidin, blue—DAPI, yellow—collagen IV).

including customized alginate [23, 24], collagen interlocked by ultra-long DNA [20], and methacrylated gelatin [22]. In our prior work using fibrin-based microgels [25, 26], we observed that preculture of microgels allowed for the formation of vessel segments within the matrix, but also resulted in the aggregation of populations of microgels into larger masses (greater than 500 μm in diameter), hindering injectability. Therefore, PEGNB microgels were subjected to extended preculture (up to 7 days) to determine if this platform could support prevascularization without microgel aggregation to develop injectable microgels. Quantification of the percentage of microgels containing primitive vessel-like structures (Figure 6E) revealed that the majority (72% ± 14%) of cell-containing microgels contained primitive vessel-like structures present throughout the matrix as early as 3 days (Figure 6A,B). These structures persisted through 7 days of preculture (80% ± 4%) (Figure 6C,D). UEA-negative phalloidin staining appeared mainly localized to the outside of the microgels, suggesting fibroblasts migrated to the exterior of the microgels as the endothelial cells assembled into vessel-like structures inside the modules.

As preculture time progressed, vessel-like structures continued to develop inside the PEGNB microgels, resulting in greater basement membrane deposition and more well-defined UEA-positive structures. Immunostaining for COL IV (Figure S2) showed an increase in the presence of the protein with increased preculture duration, indicating vessel maturation over time. Importantly, microgels cultured for up to a week in suspension showed no signs of microgel aggregation, permitting extended preculture of discrete tissue modules without compromising injectability or diffusion of nutrients into the microgels [27].

3.4 | Co-Encapsulation of Endothelial and Stromal Cells Is Required for Effective Prevascularization of Microgels

During microfluidic droplet production, we occasionally observed the formation of cell aggregates in the precursor solution (not shown), which resulted in variations in the numbers of cells per microgel across a population of microgels. Through a series of troubleshooting experiments, we determined that NHLFs were the cell type primarily responsible for these aggregates. This observation, combined with prior evidence in the literature demonstrating vessel morphogenesis in bulk PEG hydrogels containing endothelial cells alone [30], led us to assess if HUVEC monoculture microgels (20×10^6 cells/mL) could be prevascularized in the absence of stromal cells. After 5 days of suspension culture (D5 PC), HUVEC monocultures showed no evidence of vessel morphogenesis within the microgels (Figure 7A). D1 PC HUVEC monoculture microgels were embedded in bulk fibrin hydrogels containing 250 K/mL NHLF and cultured for 7 days.

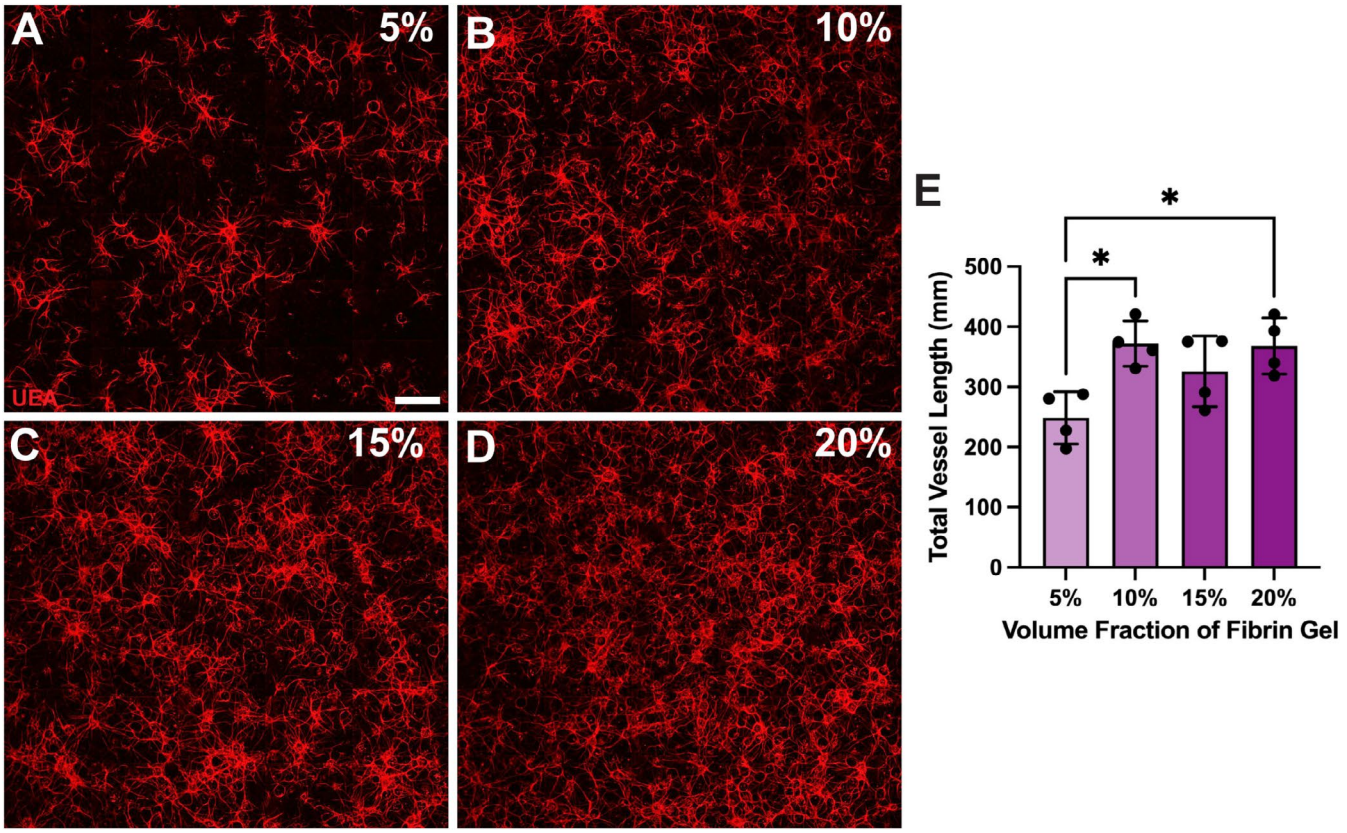

FIGURE 4 | Microgels form robust, well-distributed microvascular networks. Whole gel scan slides (10 mm × 10 mm) of 2.5 mg/mL fibrin hydrogels containing (A) 5%, (B) 10%, (C) 15%, and (D) 20% volume fraction of D1 PC cell-laden PEGNB microgels cultured for 7 days in vitro (red—UEA; scale bar = 1000 μm). (E) Quantification of total vessel length for tested volume fractions.

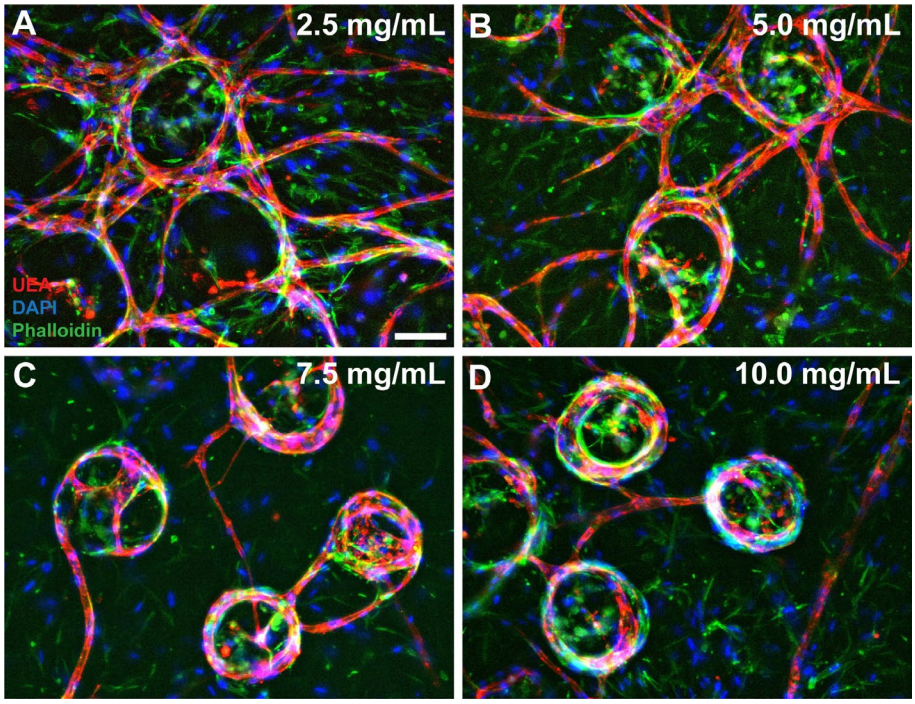

FIGURE 5 | Microgels vascularize high density fibrin hydrogels. Representative max intensity projections ($Z = 150\,\mu m$) of D1 PC microgels cultured in (A) 2.5, (B) 5.0, (C) 7.5, and (D) 10.0 mg/mL fibrin hydrogels for 7 days in vitro (red—UEA, green—phalloidin, blue—DAPI; scale bar = 100 μm).

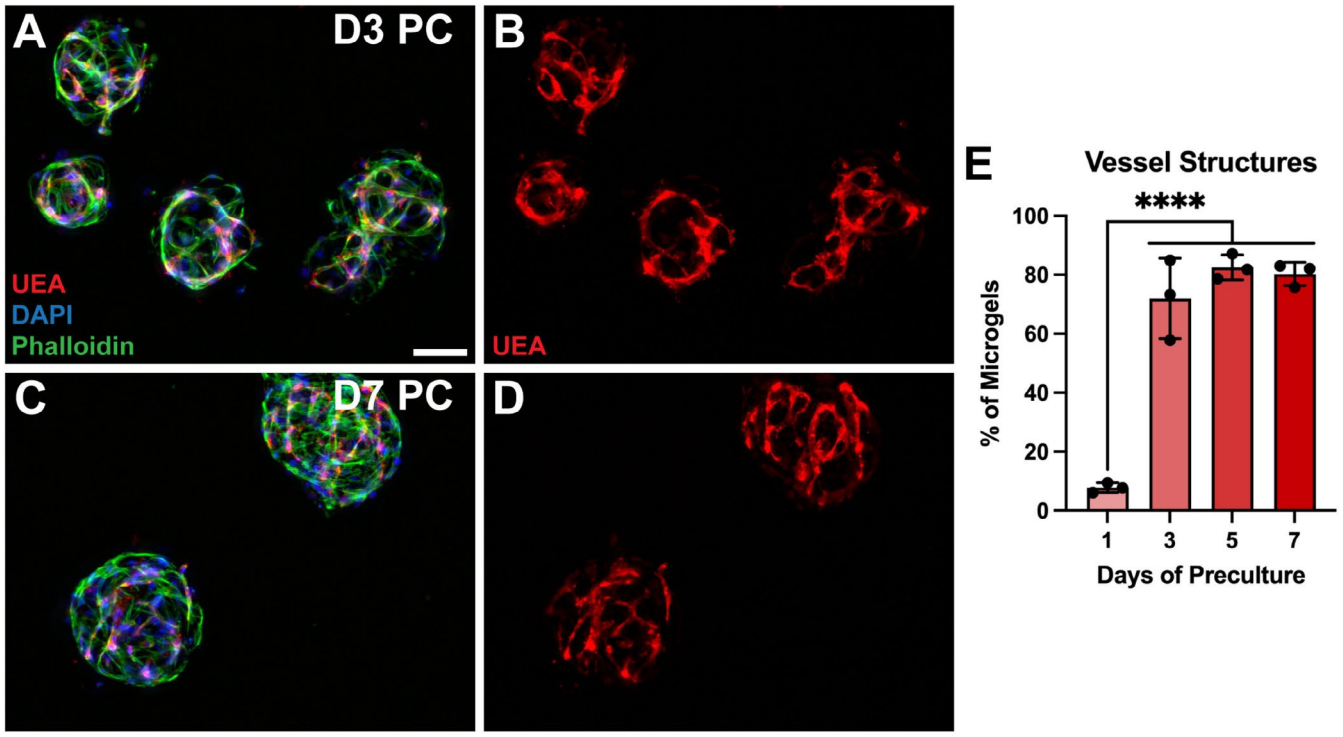

FIGURE 6 | Microgels support prevascularization through extended suspension culture. Representative max intensity projections ($Z = 100\,\mu m$) of microgels cultured in suspension for (A, B) 3 and (C, D) 7 days (red—UEA, green—phalloidin, blue—DAPI; scale bar = 100 μm). (E) Quantification of primitive vessel-like structures within cellular microgels; ****$p < 0.0001$, $N = 3$ batches.

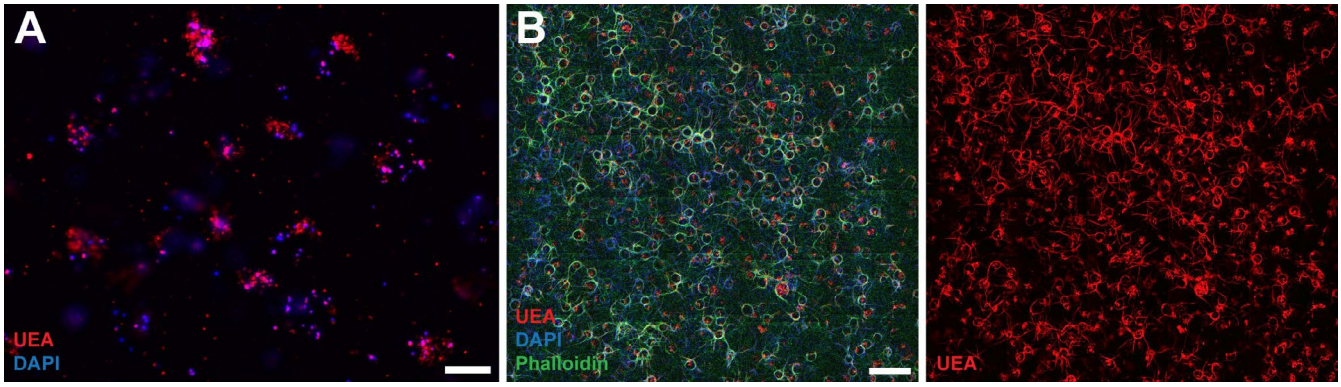

FIGURE 7 | HUVEC monoculture microgels facilitate angiogenic sprouting but lack the capability of prevascularization. (A) D5 PC EC monoculture microgels in suspension (scale bar = 200 μm) (red—UEA, green—phalloidin, blue—DAPI). (B) Whole gel scan slides of D1 PC EC monoculture microgels embedded with 250 K/mL NHLF in bulk 2.5 mg/mL fibrin hydrogels cultured for 7 days (scale bar = 1000 μm).

NHLF in the surrounding hydrogel supported angiogenic sprouting from the HUVEC monoculture microgels (Figure 7B). Total vessel length (228 mm) was comparable to that of fibrin gels containing a 5% volume fraction of D1 PC co-culture microgels (Figure 4E). Interestingly, increasing the concentration of NHLF in the surrounding bulk gel to 500 K/mL resulted in a 55% reduction in total vessel length. While HUVEC monocultures did not facilitate prevascularization in the absence of NHLF, this result suggests that the delivery of endothelial cells alone could be effective for revascularization in vivo, with the expectation that host stromal cells would aid in vessel assembly upon implantation. This approach has been demonstrated with encapsulated endothelial colony-forming cells in PEG-fibrinogen composite microgels [18, 19].

These observations suggest that stromal cells need to be in direct (or very close) contact with HUVEC monoculture microgels to support vessel morphogenesis and angiogenic sprouting. In a subsequent experiment, equal volumes of NHLF monoculture microgels and HUVEC monoculture microgels (each fabricated with 20×10^6 cells/mL) were co-cultured in suspension in a single bioreaction tube to determine if NHLF paracrine signaling would facilitate prevascularization of HUVEC microgels in a mixed population. After 7 days of suspension culture (D7 PC), a portion of HUVEC microgels showed evidence of primitive vessel-like structures when intense phalloidin staining was present on the exterior of microgels (Figure 8, arrows). Some microgels showed punctate UEA staining and weak phalloidin staining, which we interpreted as unassembled HUVEC lacking

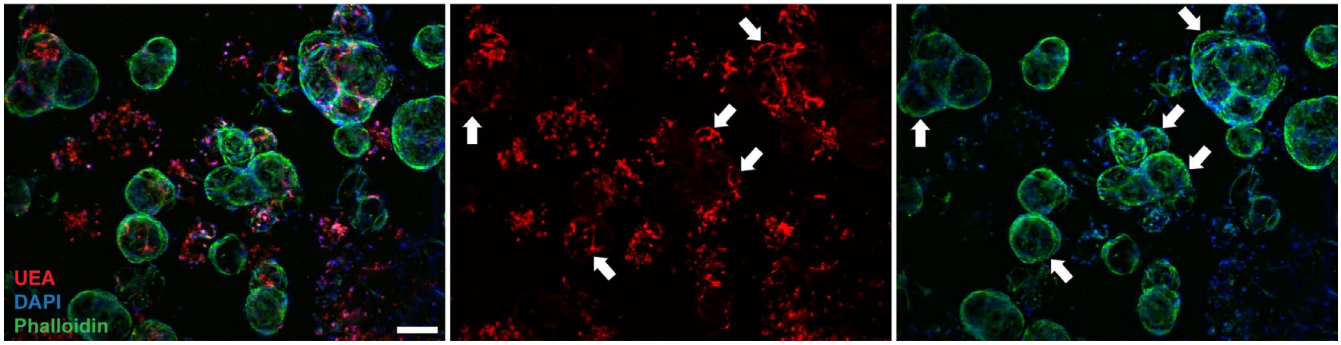

FIGURE 8 | Co-culture of HUVEC and NHLF monoculture microgels resulted in prevascularization of a portion of microgels. Monoculture microgels co-cultured in suspension in a single bioreaction tube (arrows indicate microgels that appear to contain vessel-like structures; red—UEA, green—phalloidin, blue—DAPI; scale bar = 200 μm).

actin filaments (as phalloidin should label F-actin in both cell types). Unlike microgels containing both HUVEC and NHLF, some aggregation was observed after 7 days of culture with these monoculture microgels. The prevalence of UEA-negative, phalloidin-positive microgels in these aggregates suggests the NHLF may have migrated from their microgels onto the surface of the HUVEC microgels. These findings suggest stromal cells must be in more intimate, and perhaps direct, contact with HUVEC, by way of being in/on the same microgel, for prevascularization to occur.

4 | Conclusion

Modular constructs provide discrete microenvironments that enable the delivery of functional tissue units and/or the ability to engineer complex tissue structures. In this study, we reproducibly fabricated fully synthetic RGD-modified and protease-susceptible cell-laden PEGNB microgels via microfluidic biofabrication, producing homogeneous droplets with a narrow size distribution. We showed for the first time the ability to encapsulate populations of both EC and stromal fibroblasts within these PEG microgels, which supported extended periods of suspension preculture and enabled prevascularization of individual microgels. When embedded in a surrounding hydrogel matrix, EC within these microgels were also able to sprout and form interconnected networks with those from adjacent microgels to extensively vascularize larger tissue volumes. Compared to those formulated from natural matrices, PEG-based microgels offer a "blank slate" that can be modified to include tissue-specific peptides or bioactive molecules and can be easily customized for encapsulation of different cell types to produce tissue-specific modules without changing the manner of microgel production. This approach, therefore, has the potential to be incorporated into strategies, such as modular granular scaffolds or 3D bioprinting, to promote the development of well-distributed microvascular networks throughout large volumes, increasing the complexity and functionality of engineered tissue constructs.

Author Contributions

Nicole E. Friend: conceptualization, methodology, formal analysis, investigation, data curation, writing – original draft, writing – review and editing, visualization. **Irene W. Zhang:** data curation. **Michael M. Hu:** data curation. **Atticus J. McCoy:** data curation. **Robert N. Kent III:** methodology. **Samuel J. DePalma:** methodology. **Brendon M. Baker:** resources, writing – review and editing. **Sasha Cai Lesher-Pérez:** methodology, resources, writing – review and editing. **Jan P. Stegemann:** conceptualization, resources, writing – review and editing, supervision, project administration, funding acquisition. **Andrew J. Putnam:** conceptualization, resources, data curation, writing – review and editing, supervision, project administration, funding acquisition.

Acknowledgments

Research reported in this publication was supported by the National Heart, Lung, and Blood Institute of the National Institutes of Health under Award Numbers R01-HL085339 (AJP) and R01-HL118259 (J.P.S. and A.J.P.). N.E.F. was partially supported by the Tissue Engineering and Regeneration Training Program at the University of Michigan (T32-DE007057) and the Rackham Merit Fellowship. I.W.Z was partially supported by the Cellular Biotechnology Training Program at the University of Michigan (T32-GM145304). A.J.M. was partially supported by the Training Program in Translational Cardiovascular Research and Entrepreneurship at the University of Michigan (T32-HL125242). The content is solely the responsibility of the authors and does not necessarily represent the official views of the National Institutes of Health.

Conflicts of Interest

The authors declare no conflicts of interest.

Data Availability Statement

The data that support the findings of this study are available from the corresponding author upon reasonable request.

References

1. A. J. Putnam and D. J. Mooney, "Tissue Engineering Using Synthetic Extracellular Matrices," *Nature Medicine* 2, no. 7 (1996): 824–826.

2. P. Chandra and A. Atala, "Engineering Blood Vessels and Vascularized Tissues: Technology Trends and Potential Clinical Applications," *Clinical Science* 133, no. 9 (2019): 1115–1135.

3. E. A. Margolis, N. E. Friend, M. W. Rolle, E. Alsberg, and A. J. Putnam, "Manufacturing the Multiscale Vascular Hierarchy: Progress Toward Solving the Grand Challenge of Tissue Engineering," *Trends in Biotechnology* 41 (2023): 1400–1416.

4. D. R. Griffin, W. M. Weaver, P. O. Scumpia, D. di Carlo, and T. Segura, "Accelerated Wound Healing by Injectable Microporous Gel Scaffolds Assembled From Annealed Building Blocks," *Nature Materials* 14, no. 7 (2015): 737–744.

5. A. S. Caldwell, B. A. Aguado, and K. S. Anseth, "Designing Microgels for Cell Culture and Controlled Assembly of Tissue Microenvironments," *Advanced Functional Materials* 30, no. 37 (2020): 1907670.

6. N. G. Schott, H. Vu, and J. P. Stegemann, "Multimodular Vascularized Bone Construct Comprised of Vasculogenic and Osteogenic Microtissues," *Biotechnology and Bioengineering* 119, no. 11 (2022): 3284–3296.

7. Y. Fang, Y. Guo, M. Ji, et al., "3D Printing of Cell-Laden Microgel-Based Biphasic Bioink With Heterogeneous Microenvironment for Biomedical Applications," *Advanced Functional Materials* 32, no. 13 (2022): 2109810.

8. C. E. Miksch, N. P. Skillin, B. E. Kirkpatrick, et al., "4D Printing of Extrudable and Degradable Poly(Ethylene Glycol) Microgel Scaffolds for Multidimensional Cell Culture," *Small* 18, no. 36 (2022): e2200951.

9. Y. Ou, S. Cao, Y. Zhang, et al., "Bioprinting Microporous Functional Living Materials From Protein-Based Core-Shell Microgels," *Nature Communications* 14, no. 1 (2023): 322.

10. G. Yang, B. Mahadik, J. Y. Choi, et al., "Fabrication of Centimeter-Sized 3D Constructs With Patterned Endothelial Cells Through Assembly of Cell-Laden Microbeads as a Potential Bone Graft," *Acta Biomaterialia* 121 (2021): 204–213.

11. A. Lee, A. R. Hudson, D. J. Shiwarski, et al., "3D Bioprinting of Collagen to Rebuild Components of the Human Heart," *Science* 365, no. 6452 (2019): 482–487.

12. X. Wang, X. Liu, W. Liu, et al., "3D Bioprinting Microgels to Construct Implantable Vascular Tissue," *Cell Proliferation* 56, no. 5 (2023): e13456.

13. J. K. Gandhi, L. Zivkovic, J. P. Fisher, M. C. Yoder, and E. M. Brey, "Enhanced Viability of Endothelial Colony Forming Cells in Fibrin Microbeads for Sensor Vascularization," *Sensors* 15, no. 9 (2015): 23886–23902.

14. G. Ramirez-Calderon, H. H. Susapto, and C. A. E. Hauser, "Delivery of Endothelial Cell-Laden Microgel Elicits Angiogenesis in Self-Assembling Ultrashort Peptide Hydrogels in Vitro," *ACS Applied Materials & Interfaces* 13, no. 25 (2021): 29281–29292.

15. A. Y. Rioja, E. L. H. Daley, J. C. Habif, A. J. Putnam, and J. P. Stegemann, "Distributed Vasculogenesis From Modular Agarose-Hydroxyapatite-Fibrinogen Microbeads," *Acta Biomaterialia* 55 (2017): 144–152.

16. W. J. Seeto, Y. Tian, S. Pradhan, P. Kerscher, and E. A. Lipke, "Rapid Production of Cell-Laden Microspheres Using a Flexible Microfluidic Encapsulation Platform," *Small* 15, no. 47 (2019): e1902058.

17. P. H. Kim, H. G. Yim, Y. J. Choi, et al., "Injectable Multifunctional Microgel Encapsulating Outgrowth Endothelial Cells and Growth Factors for Enhanced Neovascularization," *Journal of Controlled Release* 187 (2014): 1–13.

18. W. J. Seeto, Y. Tian, R. L. Winter, F. J. Caldwell, A. A. Wooldridge, and E. A. Lipke, "Encapsulation of Equine Endothelial Colony Forming Cells in Highly Uniform, Injectable Hydrogel Microspheres for Local Cell Delivery," *Tissue Engineering. Part C, Methods* 23, no. 11 (2017): 815–825.

19. R. L. Winter, Y. Tian, F. J. Caldwell, et al., "Cell Engraftment, Vascularization, and Inflammation After Treatment of Equine Distal Limb Wounds With Endothelial Colony Forming Cells Encapsulated Within Hydrogel Microspheres," *BMC Veterinary Research* 16, no. 1 (2020): 43.

20. H. Zhao, Z. Wang, S. Jiang, et al., "Microfluidic Synthesis of Injectable Angiogenic Microgels," *Cell Reports Physical Science* 1, no. 5 (2020): 100047.

21. P. Du, A. D. S. Da Costa, C. Savitri, S. S. Ha, P.-Y. Wang, and K. Park, "An Injectable, Self-Assembled Multicellular Microsphere With the Incorporation of Fibroblast-Derived Extracellular Matrix for Therapeutic Angiogenesis," *Materials Science & Engineering. C, Materials for Biological Applications* 113 (2020): 110961.

22. C. M. Franca, A. Athirasala, R. Subbiah, et al., "High-Throughput Bioprinting of Geometrically-Controlled Pre-Vascularized Injectable Microgels for Accelerated Tissue Regeneration," *Advanced Healthcare Materials* 12 (2023): e2202840.

23. A. L. Torres, S. J. Bidarra, M. T. Pinto, P. C. Aguiar, E. A. Silva, and C. C. Barrias, "Guiding Morphogenesis in Cell-Instructive Microgels for Therapeutic Angiogenesis," *Biomaterials* 154 (2018): 34–47.

24. A. L. Torres, S. J. Bidarra, D. P. Vasconcelos, et al., "Microvascular Engineering: Dynamic Changes in Microgel-Entrapped Vascular Cells Correlates With Higher Vasculogenic/Angiogenic Potential," *Biomaterials* 228 (2020): 119554.

25. N. E. Friend, J. A. Beamish, E. A. Margolis, N. G. Schott, J. P. Stegemann, and A. J. Putnam, "Pre-Cultured, Cell-Encapsulating Fibrin Microbeads for the Vascularization of Ischemic Tissues," *Journal of Biomedical Materials Research. Part A* 112 (2024): 549–561.

26. N. E. Friend, A. Y. Rioja, Y. P. Kong, et al., "Injectable Pre-Cultured Tissue Modules Catalyze the Formation of Extensive Functional Microvasculature In Vivo," *Scientific Reports* 10, no. 1 (2020): 15562.

27. T. L. Place, F. E. Domann, and A. J. Case, "Limitations of Oxygen Delivery to Cells in Culture: An Underappreciated Problem in Basic and Translational Research," *Free Radical Biology & Medicine* 113 (2017): 311–322.

28. X. Li, Q. Sun, Q. Li, N. Kawazoe, and G. Chen, "Functional Hydrogels With Tunable Structures and Properties for Tissue Engineering Applications," *Frontiers in Chemistry* 6 (2018): 499.

29. B. A. Juliar, J. A. Beamish, M. E. Busch, D. S. Cleveland, L. Nimmagadda, and A. J. Putnam, "Cell-Mediated Matrix Stiffening Accompanies Capillary Morphogenesis in Ultra-Soft Amorphous Hydrogels," *Biomaterials* 230 (2020): 119634.

30. A. Brown, H. He, E. Trumper, J. Valdez, P. Hammond, and L. G. Griffith, "Engineering PEG-Based Hydrogels to Foster Efficient Endothelial Network Formation in Free-Swelling and Confined Microenvironments," *Biomaterials* 243 (2020): 119921.

31. M. R. Zanotelli, H. Ardalani, J. Zhang, et al., "Stable Engineered Vascular Networks From Human Induced Pluripotent Stem Cell-Derived Endothelial Cells Cultured in Synthetic Hydrogels," *Acta Biomaterialia* 35 (2016): 32–41.

32. E. B. Peters, N. Christoforou, K. W. Leong, G. A. Truskey, and J. L. West, "Poly(Ethylene Glycol) Hydrogel Scaffolds Containing Cell-Adhesive and Protease-Sensitive Peptides Support Microvessel Formation by Endothelial Progenitor Cells," *Cellular and Molecular Bioengineering* 9, no. 1 (2016): 38–54.

33. R. M. Schweller, Z. J. Wu, B. Klitzman, and J. L. West, "Stiffness of Protease Sensitive and Cell Adhesive PEG Hydrogels Promotes Neovascularization in Vivo," *Annals of Biomedical Engineering* 45, no. 6 (2017): 1387–1398.

34. F. Jivan, R. Yegappan, H. Pearce, et al., "Sequential Thiol-Ene and Tetrazine Click Reactions for the Polymerization and Functionalization of Hydrogel Microparticles," *Biomacromolecules* 17, no. 11 (2016): 3516–3523.

35. D. G. Belair, M. J. Miller, S. Wang, et al., "Differential Regulation of Angiogenesis Using Degradable VEGF-Binding Microspheres," *Biomaterials* 93 (2016): 27–37.

36. G. A. Foster, D. M. Headen, C. González-García, M. Salmerón-Sánchez, H. Shirwan, and A. J. García, "Protease-Degradable Microgels for Protein Delivery for Vascularization," *Biomaterials* 113 (2017): 170–175.

37. S. Xin, O. M. Wyman, and D. L. Alge, "Assembly of PEG Microgels Into Porous Cell-Instructive 3D Scaffolds via Thiol-Ene Click Chemistry," *Advanced Healthcare Materials* 7, no. 11 (2018): e1800160.

38. R. Matta, S. Lee, N. Genet, K. K. Hirschi, J. L. Thomas, and A. L. Gonzalez, "Minimally Invasive Delivery of Microbeads With Encapsulated,

Viable and Quiescent Neural Stem Cells to the Adult Subventricular Zone," *Scientific Reports* 9, no. 1 (2019): 17798.

39. C. M. Ghajar, K. S. Blevins, C. C. W. Hughes, S. C. George, and A. J. Putnam, "Mesenchymal Stem Cells Enhance Angiogenesis in Mechanically Viable Prevascularized Tissues via Early Matrix Metalloproteinase Upregulation," *Tissue Engineering* 12, no. 10 (2006): 2875–2888.

40. C. M. Ghajar, X. Chen, J. W. Harris, et al., "The Effect of Matrix Density on the Regulation of 3-D Capillary Morphogenesis," *Biophysical Journal* 94, no. 5 (2008): 1930–1941.

41. J. R. Bezenah, Y. P. Kong, and A. J. Putnam, "Evaluating the Potential of Endothelial Cells Derived From Human Induced Pluripotent Stem Cells to Form Microvascular Networks in 3D Cultures," *Scientific Reports* 8, no. 1 (2018): 2671.

42. Z. Jiang, B. Xia, R. McBride, and J. Oakey, "A Microfluidic-Based Cell Encapsulation Platform to Achieve High Long-Term Cell Viability in Photopolymerized PEGNB Hydrogel Microspheres," *Journal of Materials Chemistry B* 5, no. 1 (2017): 173–180.

43. N. E. Friend, A. J. McCoy, J. P. Stegemann, and A. J. Putnam, "A Combination of Matrix Stiffness and Degradability Dictate Microvascular Network Assembly and Remodeling in Cell-Laden Poly(Ethylene Glycol) Hydrogels," *Biomaterials* 295 (2023): 122050.

44. W. L. Matochko, S. Ng, M. R. Jafari, J. Romaniuk, S. K. Y. Tang, and R. Derda, "Uniform Amplification of Phage Display Libraries in Monodisperse Emulsions," *Methods* 58, no. 1 (2012): 18–27.

45. C. Holtze, A. C. Rowat, J. J. Agresti, et al., "Biocompatible Surfactants for Water-in-Fluorocarbon Emulsions," *Lab on a Chip* 8, no. 10 (2008): 1632–1639.

46. E. A. Margolis, D. S. Cleveland, Y. P. Kong, et al., "Stromal Cell Identity Modulates Vascular Morphogenesis in a Microvasculature-On-a-Chip Platform," *Lab on a Chip* 21, no. 6 (2021): 1150–1163.

47. N. Kosyakova, D. D. Kao, M. Figetakis, et al., "Differential Functional Roles of Fibroblasts and Pericytes in the Formation of Tissue-Engineered Microvascular Networks In Vitro," *npj Regenerative Medicine* 5 (2020): 1.

48. J. M. Hughes, P. M. Budd, A. Grieve, P. Dutta, K. Tiede, and J. Lewis, "Highly Monodisperse, Lanthanide-Containing Polystyrene Nanoparticles as Potential Standard Reference Materials for Environmental "Nano" Fate Analysis," *Journal of Applied Polymer Science* 132, no. 24 (2015): 42061.

49. C. Y. Li, D. K. Wood, J. H. Huang, and S. N. Bhatia, "Flow-Based Pipeline for Systematic Modulation and Analysis of 3D Tumor Microenvironments," *Lab on a Chip* 13, no. 10 (2013): 1969–1978.

50. S. Allazetta, L. Kolb, S. Zerbib, J.̇. Bardy, and M. P. Lutolf, "Cell-Instructive Microgels With Tailor-Made Physicochemical Properties," *Small* 11, no. 42 (2015): 5647–5656.

51. M. G. A. Mohamed, S. Kheiri, S. Islam, H. Kumar, A. Yang, and K. Kim, "An Integrated Microfluidic Flow-Focusing Platform for on-Chip Fabrication and Filtration of Cell-Laden Microgels," *Lab on a Chip* 19, no. 9 (2019): 1621–1632.

52. J. M. De Rutte, J. Koh, and D. Di Carlo, "Scalable High-Throughput Production of Modular Microgels for in Situ Assembly of Microporous Tissue Scaffolds," *Advanced Functional Materials* 29, no. 25 (2019): 1900071.

53. H. Zhang, L. Zhang, C. An, et al., "Large-Scale Single-Cell Encapsulation in Microgels Through Metastable Droplet-Templating Combined With Microfluidic-Integration," *Biofabrication* 14, no. 3 (2022): 035015.

54. M. Schot, M. Becker, C. A. Paggi, et al., "Photoannealing of Microtissues Creates High-Density Capillary Network Containing Living Matter in a Volumetric-Independent Manner," *Advanced Materials* 36 (2024): e2308949.

55. L. J. Pruett, A. L. Taing, N. S. Singh, S. M. Peirce, and D. R. Griffin, "In Silico Optimization of Heparin Microislands in Microporous Annealed Particle Hydrogel for Endothelial Cell Migration," *Acta Biomaterialia* 148 (2022): 171–180.

56. Z. Ataie, S. Horchler, A. Jaberi, et al., "Accelerating Patterned Vascularization Using Granular Hydrogel Scaffolds and Surgical Micropuncture," *Small* 20, no. 8 (2023): e2307928, https://doi.org/10.1002/smll.202307928.

57. I. W. Zhang, L. S. Choi, N. E. Friend, et al., "Clickable PEG-Norbornene Microgels Support Suspension Bioprinting and Microvascular Assembly," *bioRxiv* (2024), https://doi.org/10.1101/2024.11.15.623424.

58. Z. Wang, Z. Ying, A. Bosy-Westphal, et al., "Specific Metabolic Rates of Major Organs and Tissues Across Adulthood: Evaluation by Mechanistic Model of Resting Energy Expenditure," *American Journal of Clinical Nutrition* 92, no. 6 (2010): 1369–1377.

59. H. Ge, M. Tian, Q. Pei, F. Tan, and H. Pei, "Extracellular Matrix Stiffness: New Areas Affecting Cell Metabolism," *Frontiers in Oncology* 11 (2021): 631991.

60. A. Shellard and R. Mayor, "Sculpting With Stiffness: Rigidity as a Regulator of Morphogenesis," *Biochemical Society Transactions* 51, no. 3 (2023): 1009–1021.

Supporting Information

Additional supporting information can be found online in the Supporting Information section.